

# Reactions of Laser-Ablated Palladium and Platinum Atoms with Ethylene: An Infrared Study of the Palladium Complex and Platinum Insertion Product Isolated in Solid Argon

Han-Gook Cho and Lester Andrews\*

Department of Chemistry, P.O. Box 400319, University of Virginia, Charlottesville, Virginia 22904-4319

Received: February 12, 2004; In Final Form: April 20, 2004

Reactions of laser-ablated palladium and platinum atoms with ethylene isotopomers have been carried out in excess argon during condensation at 7 K. Infrared spectra show that palladium forms a  $\pi$  complex with ethylene whereas platinum generates an insertion product. Acetylene is a major product, suggesting that  $H_2$  elimination from ethylene is also induced by the metal atom reactions. Product frequencies calculated by DFT are compared with the experimental values.

## Introduction

Palladium and platinum are two of the most important metals in catalytic reactions of unsaturated hydrocarbons. The metal complexes not only serve as models for probing the steps in catalytic hydrogenation and oligomerization reactions but also are of great interest from the viewpoint of elucidating the nature of the bonding between the olefinic C=C double bond and a metal center.<sup>1–3</sup> Numerous complexes of Pd and Pt have been reported, and many of them carry very important industrial applications.<sup>2</sup>

Ethylene complexes with metal atoms isolated in inert matrixes have been identified in the infrared spectra.<sup>4–12</sup> Ozin et al. observed four infrared absorptions of a Pd–ethylene complex through the reaction of thermally vaporized Pd atoms with ethylene in excess xenon and argon during condensation.<sup>6,7</sup> The absorptions are rather weak, and the vibrational characteristics are similar to those of the Ni–ethylene complex, which lead to the identification of the  $\pi$  complex. However, Pt complexes of ethylene have received little attention,<sup>13</sup> whereas various platinum complexes with other hydrocarbons or their cations have been identified.<sup>14,15</sup>

Activation of the C–H bond in ethylene by second-row transition-metal atoms, eventually leading to an insertion product, was theoretically investigated by Blomberg et al.<sup>16,17</sup> The coordination energy of Pd to ethylene (–30.7 kcal/mol), forming a  $\pi$  complex, is the largest among those of the second-row transition metals; however, the vinyl hydride product (insertion complex) is not much more stable than the reactants. For the early second-row transition metals, however, the reverse tendency is found.

Matrix isolation of reaction products of laser-ablated Pd atoms and acetylene, including 1:2 and 2:1  $\pi$  complexes, has recently been carried out in our laboratory.<sup>18</sup> In a similar study of Pt atoms and acetylene, a vinylidene, a C–H insertion, and a  $\pi$ -type complex are identified in the infrared spectrum, but PtCCH<sub>2</sub> is the major product.<sup>19</sup> More recently, the reaction of laser-ablated Zr and ethylene has been investigated, and intermediates in the  $H_2$  elimination reaction of Zr and ethylene have been identified in an argon matrix.<sup>20</sup>

Here, we report reactions of laser-ablated Pd and Pt atoms with ethylene in excess argon. The metal–ethylene complexes

are characterized through matrix infrared spectra. The vibrational characteristics of the product absorptions are confirmed by isotopic substitution and DFT calculations. Interestingly enough, acetylene is also produced, and other weak reaction products are identified in the infrared spectra.

## Experimental and Computational Methods

Laser-ablated palladium and platinum atoms were reacted with C<sub>2</sub>H<sub>4</sub>, C<sub>2</sub>D<sub>4</sub>, <sup>13</sup>C<sub>2</sub>H<sub>4</sub> (Cambridge Isotope Laboratories, 99%), and CH<sub>2</sub>CD<sub>2</sub> (MSD isotopes) in excess argon during condensation at 7 K using a closed-cycle He refrigerator (Air Products HC-2). The methods are described in detail elsewhere.<sup>21–24</sup> Concentrations of gas mixtures range from 0.25 to 5% but in most cases are typically 0.5% in argon. After the reaction, infrared spectra were recorded at a resolution of 0.5 cm<sup>–1</sup> using a Nicolet 550 spectrometer with a HgCdTe detector. Later, samples were annealed, and more spectra were recorded.

Complementary density functional theory (DFT) calculations were carried out using the Gaussian 98 package,<sup>25</sup> B3LYP density functional, 6-311+G(2d,p) basis sets for C, H, and the LanL2 pseudopotential, and LanL2DZ basis set for Pd and Pt to provide a consistent set of vibrational frequencies for the reaction products. The geometries were fully relaxed during optimization, and the nature of the stationary states is confirmed by vibrational analysis. All of the vibrational frequencies were calculated analytically. In the calculation of the binding energy of a metal complex, the zero-point energy is included.

## Results and Discussion

The contrasting chemistry of palladium and platinum is illustrated in their different reaction products with ethylene.

**Pd–Ethylene Complex.** Figure 1 shows the infrared spectra in the regions of 1000–1550 and 450–1000 cm<sup>–1</sup> of laser-ablated Pd atoms codeposited with ethylene isotopomers in excess argon at 7 K, and the observed frequencies of the product absorptions indicated with arrows are summarized along with the calculated values in Table 1. The very weak absorptions at 1505.1 cm<sup>–1</sup> for C<sub>2</sub>H<sub>4</sub> shows <sup>12</sup>C/<sup>13</sup>C and H/D shifts of –20 and –173 cm<sup>–1</sup> (<sup>12</sup>C/<sup>13</sup>C and H/D isotopic ratios of 1.013 and 1.129). The absorption becomes much stronger in the spectrum of Pd + CH<sub>2</sub>CD<sub>2</sub>, as shown in Figure 1. The isotopic shifts indicate that the absorptions originate from a vibrational mode

\* Corresponding author. E-mail: lsa@virginia.edu.

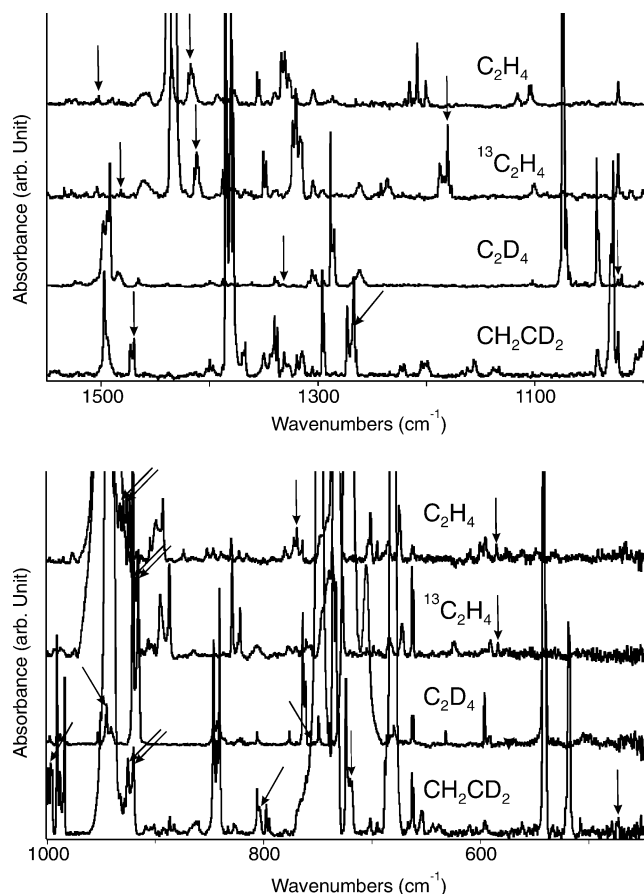


**Figure 1.** IR spectra in the regions of 1000–1550 and 450–1000  $\text{cm}^{-1}$  for laser-ablated Pd atoms codeposited with ethylene isotopomers diluted in argon at 7 K. The product absorptions marked with arrows are believed to arise from the  $\pi$  complex of Pd and ethylene isotopomers.

where the C=C stretching and  $\text{CH}_2$  deformation are strongly coupled; therefore, they are attributed to the  $\nu_2$   $A_1$   $\nu(\text{CC}) + \delta(\text{CH}_2)$  mode.

The C=C stretching mode of the  $\pi$  complex is accompanied by a small change in the dipole moment along the  $C_{2v}$  molecular axis. As a result, the C=C stretching mode, which is originally IR inactive for ethylene, becomes active in the  $\pi$  complex; however, the intensity is expected to be very low. The weak product absorptions near 1505  $\text{cm}^{-1}$  are consistent with the expected vibrational characteristics of the  $\pi$  complex.

The relatively strong absorptions at  $\sim 1418 \text{ cm}^{-1}$  show very small  $^{12}\text{C}/^{13}\text{C}$  and large H/D shifts of  $-5$  and  $-365 \text{ cm}^{-1}$  ( $^{12}\text{C}/^{13}\text{C}$  and H/D isotopic ratios of 1.003 and 1.385, respectively). They are attributed to the  $\nu_{13}$   $B_2$   $\text{CH}_2$  scissoring mode, whereas the absorptions at about 1215  $\text{cm}^{-1}$  show a much larger  $^{12}\text{C}/^{13}\text{C}$  shift of  $-35 \text{ cm}^{-1}$  and a smaller H/D shift of  $-269 \text{ cm}^{-1}$  ( $^{12}\text{C}/^{13}\text{C}$  and H/D isotopic ratios of 1.024 and 1.285), indicating that the absorptions originate from a vibrational mode where the C=C stretching and  $\text{CH}_2$  deformation are strongly coupled, similar to those of the  $\nu_2$  band. They are assigned to the  $\nu_3$   $A_1$   $\delta(\text{CH}_2) + \nu(\text{CC})$  mode. Strong coupling of the C=C stretching and  $\text{CH}_2$  scissoring for the  $\nu_2$  and  $\nu_3$  modes is a typical characteristic of a metal–ethylene  $\pi$  complex as discussed in previous studies.<sup>6,7</sup> The strongest product absorptions are observed at  $\sim 928 \text{ cm}^{-1}$  with  $^{12}\text{C}/^{13}\text{C}$  and H/D shifts of  $-10$  and  $-191 \text{ cm}^{-1}$  ( $^{12}\text{C}/^{13}\text{C}$  and H/D isotopic ratios of 1.011 and 1.258), which are attributed to the  $\nu_{14}$   $B_2$   $\text{CH}_2$  wagging mode.

Ozin and Power conducted first the reaction of thermally evaporated Pd and ethylene isotopomers ( $\text{C}_2\text{H}_4$ ,  $\text{C}_2\text{D}_4$ , and  $^{13}\text{C}_2\text{H}_4$ ) and observed four bands from each isotopomer.<sup>6,7</sup> The product absorptions were compared with those of the Ni–ethylene complex;<sup>5,10,11</sup> they concluded on the basis of the characteristics of the observed bands that the Pd atom forms a  $\pi$  complex with ethylene. To compensate for the weak infrared absorptions of the metal–ethylene complex, the concentrations of the reactants in their experiments were relatively high.

The  $\pi$  complex has 15 vibrational modes, 12 of which are infrared active except for the 3  $A_2$  modes. The hydrogen stretching absorptions of the complex are not observed in this study, in part because of the fact that the hydrogen stretching region is dominated by much stronger broad absorptions of ethylene in the matrix spectrum. The frequencies of the  $\nu_2$  absorptions ( $A_1$ ) shown in Table 1 are almost identical to the previously reported value by Ozin and Power (1502  $\text{cm}^{-1}$ ); however, the  $\nu_3$  and  $\nu_{14}$  absorptions differ by 5–15  $\text{cm}^{-1}$  from the previous values.<sup>6,7</sup> The relatively high concentrations of ethylene in argon (up to 10%) used in the previous study might cause frequency shifts due to molecular interactions with the products. In addition, we observe three weaker modes,  $\nu_{10}$ ,  $\nu_{11}$ , and  $\nu_{13}$ , not reported by the Ozin group, and we employ the lower-symmetry  $\text{CH}_2\text{CD}_2$  isotopic precursor molecule, which provides additional vibrational information including the enhancement of the mostly C–C stretching mode intensity.

DFT calculations were carried out for the  $\pi$  complex at the B3LYP/6-311+G(2d,p) and LanL2DZ levels. The optimized  $^1A_1$

**TABLE 1: Observed and B3LYP Calculated Frequencies of the Fundamental Bands of the Pd–Ethylene Complex ( $^1A_1$  State)<sup>a</sup>**

| description  | Pd( $\text{C}_2\text{H}_4$ )        |        |     | $\text{C}_2\text{H}_4$ |        | Pd( $\text{C}_2\text{D}_4$ ) |     | Pd( $^{13}\text{C}_2\text{H}_4$ )   |        |     | Pd( $\text{CH}_2\text{CD}_2$ ) |        |     |
|--|-------------------------------------|--------|-----|------------------------|--------|------------------------------|-----|-------------------------------------|--------|-----|--------------------------------|--------|-----|
|  | exptl                               | calcd  | int | calcd                  | exptl  | calcd                        | int | exptl                               | calcd  | int | exptl                          | calcd  | int |
| $\nu_1$ $A_1$ $\text{CH}_2$ s. str.                  |                                     | 3114.7 | 5   | 3136.6                 |        | 2279.8                       | 1   |                                     | 3108.1 | 5   |                                | 3111.0 | 8   |
| $\nu_2$ $A_1$ $\nu(\text{CC}) + \delta(\text{CH}_2)$ | <b>1505.1</b> , <sup>b</sup> 1502.4 | 1555.5 | 1   | 1686.7                 | 1330.6 | 1374.5                       | 4   | <b>1485.3</b> , <sup>b</sup> 1482.4 | 1533.3 | 0   | 1470.0                         | 1520.1 | 2   |
| $\nu_3$ $A_1$ $\delta(\text{CH}_2) + \nu(\text{CC})$ | 1216.4, 1208.7                      | 1248.2 | 7   | 1379.8                 | 946.5  | 966.2                        | 2   | 1188.0, 1180.3                      | 1219.2 | 7   | 999.3, 995.5                   | 1018.8 | 3   |
| $\nu_4$ $A_1$ $\text{CH}_2$ rock                     | 933.9                               | 940.6  | 3   | 973.4                  |        | 699.7                        | 0   | 922.4                               | 937.1  | 3   | 720.8                          | 733.1  | 6   |
| $\nu_5$ $A_1$ $\text{PdC}_2$ s. str.                 |                                     | 363.0  | 7   |                        |        | 350.1                        | 7   |                                     | 352.5  | 7   |                                | 361.0  | 6   |
| $\nu_6$ $A_2$ $\text{CH}_2$ str.                     |                                     | 3178.7 | 0   | 3193.8                 |        | 2370.2                       | 0   |                                     | 3165.8 | 0   |                                | 2376.5 | 1   |
| $\nu_7$ $A_2$ $\text{CH}_2$ rock                     |                                     | 1228.6 | 0   | 1247.4                 |        | 984.6                        | 0   |                                     | 1213.6 | 0   |                                | 1135.3 | 0   |
| $\nu_8$ $A_2$ $\text{CH}_2$ twist.                   |                                     | 942.1  | 0   | 1057.5                 |        | 672.9                        | 0   |                                     | 940.7  | 0   | 804.4                          | 840.6  | 1   |
| $\nu_9$ $B_1$ $\text{CH}_2$ a. str.                  |                                     | 3202.2 | 7   | 3221.9                 |        | 2382.6                       | 3   |                                     | 3189.1 | 7   |                                | 3190.6 | 4   |
| $\nu_{10}$ $B_1$ $\text{CH}_2$ rock                  | 769.5                               | 822.6  | 0   | 838.4                  |        | 590.9                        | 0   |                                     | 821.5  | 0   |                                | 670.0  | 0   |
| $\nu_{11}$ $B_1$ $\text{PdCH}$ bend                  | 585                                 | 558.8  | 10  |                        |        | 404.8                        | 7   | 584                                 | 557.8  | 10  | 474                            | 450.9  | 6   |
| $\nu_{12}$ $B_2$ $\text{CH}_2$ str.                  |                                     | 3107.3 | 10  | 3124.0                 |        | 2244.5                       | 4   |                                     | 3102.4 | 10  |                                | 2262.5 | 3   |
| $\nu_{13}$ $B_2$ $\text{CH}_2$ scis.                 | 1420.1, 1417.1                      | 1465.5 | 7   | 1478.5                 | 1052.9 | 1085.0                       | 5   | 1414.5, 1412.5                      | 1459.8 | 7   | 1267.2                         | 1308.6 | 7   |
| $\nu_{14}$ $B_2$ $\text{CH}_2$ wag                   | 930.1, 926.8                        | 950.2  | 27  | 976.2                  | 736.6  | 765.7                        | 14  | 920.4, 916.8                        | 940.0  | 27  | 925.9, 920.8                   | 946.0  | 16  |
| $\nu_{15}$ $B_2$ $\text{PdC}_2$ a. str.              |                                     | 353.6  | 3   |                        |        | 318.4                        | 3   |                                     | 343.1  | 2   |                                | 330.8  | 3   |

<sup>a</sup> Frequencies are in  $\text{cm}^{-1}$ ; calculated intensities are in  $\text{km/mol}$ . Calculated frequencies listed for  $\text{C}_2\text{H}_4$  by the Pd( $\text{C}_2\text{H}_4$ ) mode derived therefrom.

<sup>b</sup> Bold denotes the surviving matrix site on annealing.

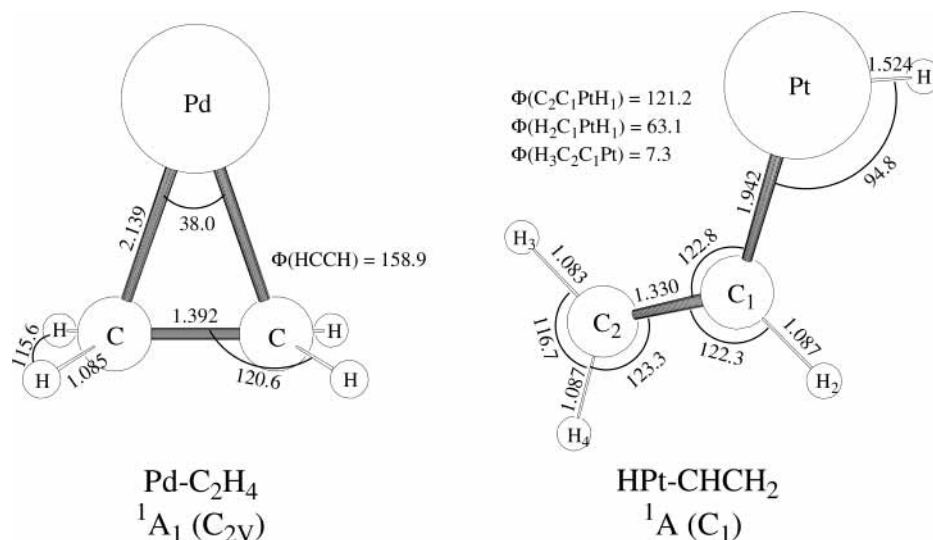


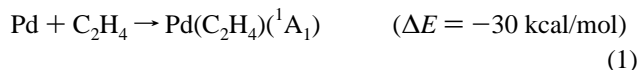
**Figure 2.** Optimized molecular structures of the  $\pi$  complex of Pd and ethylene and the insertion complex of Pt and ethylene in their ground electronic states. The bond lengths and angles are measured in angstroms and degrees, respectively. Some of the dihedral angles ( $\Phi$ ) are also shown.

**TABLE 2: Geometrical Parameters and Physical Constants Calculated for Pd and Pt Complexes with Ethylene<sup>a</sup>**

| parameters               | $\text{C}_2\text{H}_4$ | $\text{Pd-C}_2\text{H}_4$ | $\text{HPt-CHCH}_2$       |
|--------------------------|------------------------|---------------------------|---------------------------|
| $r(\text{C-C})$          | 1.325                  | 1.392                     | 1.330                     |
| $r(\text{C-H})$          | 1.084                  | 1.085                     | 1.087, 1.083, 1.087       |
| $r(\text{C-M})$          |                        | 2.139                     | 1.942                     |
| $r(\text{M-H})$          |                        |                           | 1.524                     |
| $\angle\text{CCH}$       | 121.7                  | 120.6                     | 122.8, 123.3              |
| $\angle\text{HCH}$       | 116.6                  | 115.6                     | 116.7                     |
| $\angle\text{CMC}$       |                        | 38.0                      |                           |
| $\angle\text{CMH}$       |                        |                           | 94.8                      |
| $\Phi(\text{HCCM})$      |                        | 100.6                     | 7.3                       |
| $\Phi(\text{HCMH})$      |                        |                           | 63.1                      |
| $\Phi(\text{HCCH})$      |                        | 0.0, 158.9                | 2.9, 177.2                |
| $\Phi(\text{CCMH})$      |                        |                           | 121.2                     |
| $q(\text{C})^{b,c}$      |                        | -0.19                     | -0.34, -0.23              |
| $q(\text{H})^{b,c}$      |                        | 0.10                      | -0.03, -0.10, -0.10, 0.10 |
| $q(\text{M})^b$          |                        | 0.01                      | 0.23                      |
| $\mu^d$                  | 0.00                   | 0.79                      | 0.81                      |
| $\Delta E(\pi)^e$        |                        | 30.2                      | 63.5                      |
| $\Delta E(\text{ins})^f$ |                        | 2.2                       | 55.4                      |

<sup>a</sup> B3LYP bond lengths and angles are measured in angstroms and degrees, respectively. <sup>b</sup> Mulliken atomic charge. <sup>c</sup> The first value is the value of the atom closest to the metal atom. <sup>d</sup> Molecular dipole moment in D. <sup>e</sup> Binding energy for  $\pi$  complex measured in kcal/mol. <sup>f</sup> Binding energy for insertion product measured in kcal/mol.

structure is shown in Figure 2, and the geometrical parameters are listed in Table 2. The calculated frequencies are compared with the observed values in Table 1, showing very good agreement. This result reconfirms the conclusion in earlier studies that Pd forms a  $\pi$  complex with ethylene,<sup>6,7</sup> which is also consistent with the result of the earlier theoretical studies about activation of the C-H bond in ethylene by a second-row transition-metal atom.<sup>16,17</sup> Coordination of the Pd atom to ethylene is energetically very favorable, but C-H insertion is not.



It has been reported that early second-row transition metals form metallacyclopropanes, whereas the late ones form  $\pi$  complexes.<sup>26,27</sup> They are called metallacyclopropanes because the C=C bond is weakened so much upon formation of the

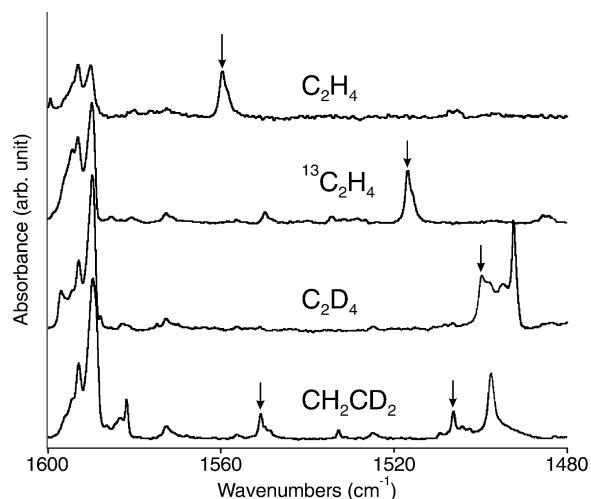


**Figure 3.** IR spectra in the region of 1480–1600  $\text{cm}^{-1}$  for laser-ablated Pt atoms codeposited with  $\text{Ar}/\text{C}_2\text{H}_4$  at 7 K. The absorptions marked with arrows are believed to originate from the C=C stretching mode of the Pt-ethylene insertion product. Note the large  ${}^{12}\text{C}/{}^{13}\text{C}$  isotopic shift.

complex that the C=C bond length approaches that of a C-C single bond. As shown in Table 2 and Figure 2, the C=C bond length of the Pd-ethylene complex is 1.39 Å, not much longer than that of a normal C=C bond (1.34 Å), indicating that the complex is a typical metal-ethylene  $\pi$  complex.

**Pt-Ethylene Insertion Product.** Shown in Figure 3 is the infrared spectra in the range of 1480–1600  $\text{cm}^{-1}$  of laser-ablated Pt atoms codeposited with ethylene isotopomers diluted in Ar at 7 K. The absorption at 1559.7  $\text{cm}^{-1}$  shows a very large  ${}^{12}\text{C}/{}^{13}\text{C}$  shift of  $-42.8 \text{ cm}^{-1}$  and a relatively small H/D shift of  $-59.9 \text{ cm}^{-1}$  ( ${}^{12}\text{C}/{}^{13}\text{C}$  and H/D isotopic ratios of 1.028 and 1.040), indicating that it is the C=C stretching absorption of a Pt- $\text{C}_2\text{H}_4$  reaction product. It is also notable that the product absorptions, marked with arrows, are quite strong, unlike the ones observed in the Pd + ethylene spectra in the same C=C stretching region.

The frequencies are also much higher than those of the CC stretching absorptions expected for a normal metal-ethylene  $\pi$  complex.<sup>6–12</sup> Calculations indicate that the C=C stretching band of the Pt- $\text{C}_2\text{H}_4$   $\pi$  complex would appear below 1500  $\text{cm}^{-1}$

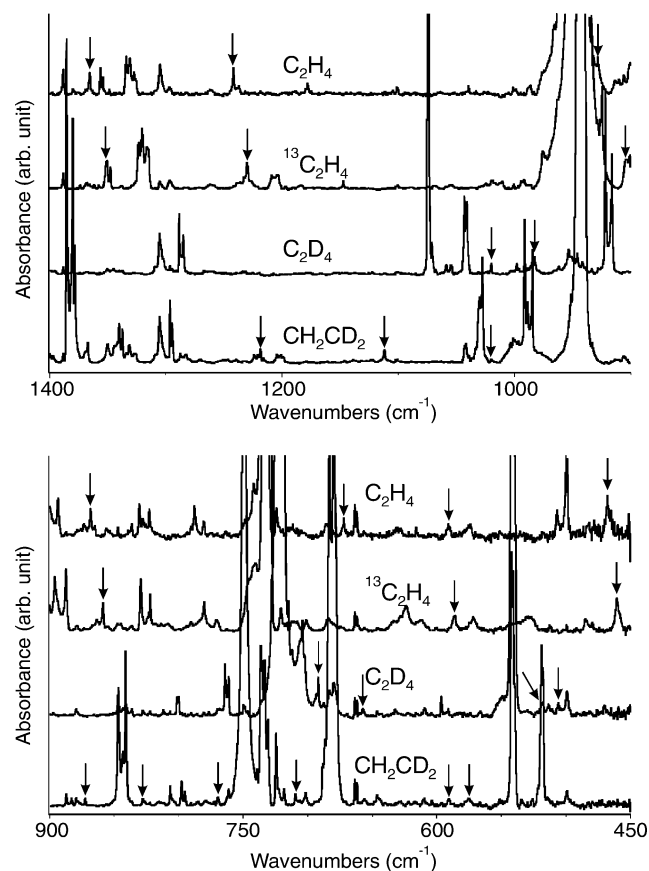


**Figure 4.** IR spectra in the regions of 950–1400 and 450–900  $\text{cm}^{-1}$  for laser-ablated Pt atoms codeposited with ethylene isotopomers diluted in argon at 7 K. The product absorptions marked with arrows are believed to arise from the insertion complexes of Pt and ethylene isotopomers.

with lower absorption intensity. The characteristics of the product absorptions in Figure 3 suggest that they in fact originate from the C=C stretching mode of a C-H insertion product of Pt and ethylene,  $\text{HPt-CHCH}_2$ . The C=C bond becomes polarized upon Pt insertion, yielding a larger change in dipole moment on stretching of the bond, which in turn leads to a stronger absorption than in the  $\pi$  complex. Earlier studies also show that Pt often makes insertion products with hydrocarbons.<sup>14,15,19</sup>

Shown in Figure 4 are the infrared spectra in the regions of 900–1400 and 450–900  $\text{cm}^{-1}$  of laser-ablated Pt atoms codeposited with ethylene isotopomers diluted in Ar at 7 K, and the frequencies of the product absorptions marked with arrows are summarized in Table 3. The product bands are, in general, much stronger than those of the  $\pi$  complexes of Pd and ethylene isotopomers.

The product absorption at 1365.6  $\text{cm}^{-1}$  show relatively small  $^{12}\text{C}/^{13}\text{C}$  and large H/D shifts of  $-13.9$  and  $-345.9$   $\text{cm}^{-1}$  ( $^{12}\text{C}/^{13}\text{C}$  and H/D isotopic ratios of 1.010 and 1.339, respectively). However, the absorption at 1242.1  $\text{cm}^{-1}$  shows a similar  $^{12}\text{C}/^{13}\text{C}$  shift of  $-11.9$   $\text{cm}^{-1}$  and a little smaller shift of  $-259.5$   $\text{cm}^{-1}$  ( $^{12}\text{C}/^{13}\text{C}$  and H/D isotopic ratios of 1.010 and 1.264, respectively). On the basis of the frequencies and the isotopic shifts, the absorptions at 1365.6 and 1242.1  $\text{cm}^{-1}$  are assigned to the  $\text{CH}_2$  scissoring and the CCH in-plane bending modes, respectively. Another product absorption at 928.0  $\text{cm}^{-1}$  with very small  $^{12}\text{C}/^{13}\text{C}$  and very large H/D isotopic shifts of  $-3.6$  and  $-270.4$   $\text{cm}^{-1}$  ( $^{12}\text{C}/^{13}\text{C}$  and H/D isotopic ratios of 1.004 and 1.411, respectively) is assigned to the HCCH out-of-plane bending mode as shown in Table 3.

The observed frequencies are compared with the calculated values for the C-H insertion complex in Table 3, and the agreement is very good. The optimized structure of the singlet insertion product ( $\text{C}_1$ ) is shown in Figure 2, and the geometrical parameters are listed in Table 2. The complex is planar except for the H on platinum. The Pt atom is located slightly above the  $\text{C}_2\text{H}_3$  molecular plane, and the hydrogen atom bonded to the metal atom is below the plane. Figure 2 also shows that the bond angle  $\angle\text{CptH}$  ( $94.8^\circ$ ) is close to a right angle.

The Pt atom is much heavier than the other atoms in the molecule. Therefore, it is expected from the molecular structure of the insertion complex that the Pt-H stretching mode is almost completely isolated from the other vibrational modes of the complex, resulting in nearly identical metal-hydrogen stretching frequencies regardless of isotopomer. Figure 5 shows the Pt-H and Pt-D stretching regions of the insertion complexes of the ethylene isotopomers. The complexes of  $\text{C}_2\text{H}_4$ ,  $^{13}\text{C}_2\text{H}_4$ , and  $\text{CH}_2\text{-CD}_2$  with Pt all have essentially the same Pt-H stretching frequencies, and those of  $\text{C}_2\text{D}_4$  and  $\text{CH}_2\text{CD}_2$  also give the same Pt-D stretching frequencies.

The present results indicate that unlike the Pd atom the Pt atom readily forms an insertion product with ethylene. Calculations are also carried out for a  $\pi$  complex of Pt and ethylene,

**TABLE 3: Observed and Calculated Frequencies of the Fundamental Bands of the  $\text{HPt-CHCH}_2$  Insertion Product ( $^1\text{A State}$ )<sup>a</sup>**

| description                      | $\text{C}_2\text{H}_4$ |        |     | $\text{C}_2\text{D}_4$ |        |     | $^{13}\text{C}_2\text{H}_4$ |        |     | $\text{CH}_2\text{CD}_2$ |        |     |                     |        |     |
|----------------------------------|------------------------|--------|-----|------------------------|--------|-----|-----------------------------|--------|-----|--------------------------|--------|-----|---------------------|--------|-----|
|                                  | exptl                  | calcd  | int | exptl                  | calcd  | int | exptl                       | calcd  | int | $\text{HPt-CHCD}_2$      |        |     | $\text{DPt-CDCH}_2$ |        |     |
|                                  |                        |        |     |                        |        |     |                             |        |     | exptl                    | calcd  | int | exptl               | calcd  | int |
| $\nu_1$ $\text{CH}_2$ asym. str. |                        | 3202.7 | 2   |                        | 2382.7 | 1   |                             | 3190.2 | 3   |                          | 2272.4 | 0   |                     | 3202.1 | 2   |
| $\nu_2$ C-H str.                 |                        | 3134.4 | 3   |                        | 2324.0 | 1   |                             | 3124.3 | 3   |                          | 3132.0 | 2   |                     | 3112.3 | 2   |
| $\nu_3$ $\text{CH}_2$ symm. str. |                        | 3109.0 | 1   |                        | 2261.4 | 1   |                             | 3102.6 | 1   |                          | 2419.8 | 1   |                     | 2313.8 | 1   |
| $\nu_4$ Pt-H str.                | 2317.7                 | 2419.8 | 14  | 1663.0                 | 1716.3 | 8   | 2317.7                      | 2419.8 | 14  | 2317.7                   | 2382.6 | 14  | 1663.0              | 1716.3 | 8   |
| $\nu_5$ C=C str.                 | 1559.7                 | 1607.5 | 44  | 1499.8                 | 1532.0 | 48  | 1516.9                      | 1560.0 | 38  | 1506.2                   | 1547.6 | 52  | 1550.8              | 1594.8 | 41  |
| $\nu_6$ $\text{CH}_2$ scis.      | 1365.6                 | 1404.4 | 21  | 1019.8                 | 1058.7 | 24  | 1351.7                      | 1389.4 | 24  | 1218.8                   | 1226.0 | 62  | 1367.5              | 1399.1 | 18  |
| $\nu_7$ CCH IP bend              | 1242.1                 | 1254.8 | 59  | 982.6                  | 996.4  | 28  | 1230.2                      | 1242.2 | 57  | 1023.0                   | 1037.7 | 3   | 1111.9              | 1123.0 | 39  |
| $\nu_8$ $\text{CH}_2$ rock       |                        | 990.3  | 8   | 691.9                  | 737.7  | 5   |                             | 983.8  | 9   | 827.9                    | 851.8  | 9   | 785.2               | 817.4  | 10  |
| $\nu_9$ HCCH OOP bend            | 928.0                  | 962.5  | 24  | 657.6                  | 707.4  | 29  | 924.4                       | 959.3  | 23  | 872.5                    | 903.9  | 17  | 772.8               | 801.0  | 3   |
| $\nu_{10}$ $\text{CH}_2$ wag     | 868.5                  | 914.6  | 30  |                        | 748.0  | 5   | 858.9                       | 903.8  | 30  | 709.7                    | 735.6  | 22  | 879.5               | 919.5  | 46  |
| $\nu_{11}$ CpH bend              | 672.0                  | 679.7  | 33  | 505.9                  | 505.5  | 17  |                             | 674.5  | 33  | 590.9                    | 636.9  | 38  | 575.0               | 601.5  | 17  |
| $\nu_{12}$ Pt-C str.             | 590.9                  | 604.8  | 10  | 518.0                  | 552.0  | 4   | 586.2                       | 588.7  | 10  |                          | 560.2  | 4   |                     | 557.0  | 15  |
| $\nu_{13}$ PtCC OOP bend         | 468                    | 466.1  | 23  |                        | 348.1  | 11  | 461                         | 463.3  | 23  |                          | 381.9  | 15  |                     | 385.8  | 12  |
| $\nu_{14}$ PtCC bend             |                        | 276.2  | 8   |                        | 238.3  | 8   |                             | 269.9  | 8   |                          | 251.3  | 7   |                     | 262.8  | 10  |
| $\nu_{15}$ HPtCH distort         |                        | 198.1  | 7   |                        | 143.4  | 3   |                             | 197.4  | 7   |                          | 195.9  | 8   |                     | 143.8  | 3   |

<sup>a</sup> Frequencies are measured in  $\text{cm}^{-1}$ ; calculated intensities are measured in  $\text{km/mol}$ .

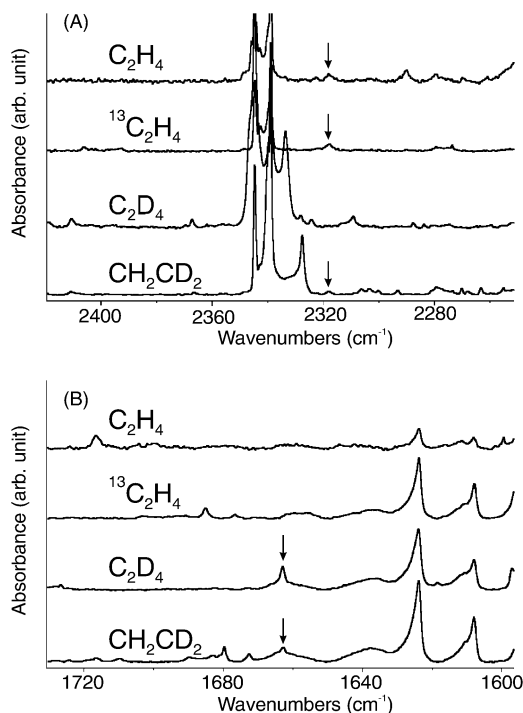
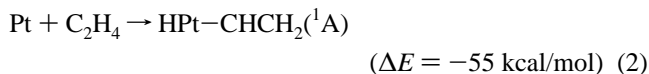


**Figure 5.** IR spectra in the Pt–H (A) and Pt–D (B) stretching regions for laser-ablated Pt atoms codeposited with ethylene isotopomers diluted in argon at 7 K. Note that the Pt–H stretching frequencies of the complexes of C<sub>2</sub>H<sub>4</sub>, <sup>13</sup>C<sub>2</sub>H<sub>4</sub>, and CH<sub>2</sub>CD<sub>2</sub> are the same and so are the Pt–D stretching frequencies of the complexes of C<sub>2</sub>D<sub>4</sub> and CH<sub>2</sub>CD<sub>2</sub>.

and with the help of the results, the complex was searched in the infrared spectrum, but there was no trace of the  $\pi$  complex. Table 2 shows that the binding energy of the insertion product relative to the reactants is slightly smaller than that of the  $\pi$  complex at the present level of theory. The absence of absorptions by a  $\pi$  complex of Pt and ethylene remains as an unsolved problem at the moment. A possible explanation is the weak infrared absorption intensities predicted for its fundamental vibrations. Similarly, the  $\pi$  complexes of Zr and Ti atoms with ethylene are not identified, whereas strong absorptions of the insertion products are observed after light irradiation in the matrix infrared spectra.<sup>20,28</sup> Another rationale is that any Pt  $\pi$  complex formed undergoes spontaneous or photoinduced rearrangement to HPtC<sub>2</sub>H<sub>3</sub>.



**Other Reaction Products.** Whereas Pd and Pt atoms, as described above, form a  $\pi$  complex and an insertion product, respectively, with ethylene during codeposition, various other reaction products are also formed. The observed frequencies listed in Tables 4 and 5 are weaker versions of the products in the reaction of Pd and Pt with acetylene.<sup>18,19</sup> However, a vinylidene complex is identified in the spectrum of Pt and ethylene, which is the major reaction product of Pt and acetylene.<sup>19</sup> Although PdH is observed, we find no evidence for PtH or PtH<sub>2</sub>.<sup>29,30</sup> Unfortunately, Pd(H<sub>2</sub>) and Pd(D<sub>2</sub>) are masked by C<sub>2</sub>H<sub>4</sub> and C<sub>2</sub>D<sub>4</sub>, but Pd(HD) is observed at 804.1 cm<sup>-1</sup>, and it grows on annealing as found previously.<sup>29</sup>

Among the product absorptions, in both Pd and Pt spectra, the strongest absorptions observed arise from acetylene (Figure 6). Normally, about 20% or more of ethylene is converted to acetylene in the present experiment for both Pd and Pt estimated from the hydrogen stretching absorptions. This result also

**TABLE 4: Observed Frequencies (cm<sup>-1</sup>) of Reaction Products Other than the  $\pi$  Complex of Pd and Ethylene<sup>a</sup>**

| species  | C <sub>2</sub> H <sub>4</sub> | C <sub>2</sub> D <sub>4</sub> | <sup>13</sup> C <sub>2</sub> H <sub>4</sub> | CH <sub>2</sub> CD <sub>2</sub> |        |        |
|--|-------------------------------|-------------------------------|---|---------------------------------|--------|--------|
| Pd(C <sub>2</sub> H <sub>2</sub> ) <sub>2</sub>  | 3184.2                        |                               |   |                                 |        |        |
| Pd(C <sub>2</sub> H <sub>2</sub> )               | 3163.8                        |                               |   |                                 |        |        |
| Pd(C <sub>2</sub> H <sub>2</sub> )               | 3153.7                        |                               |   |                                 |        |        |
| PdH  | 1952.8                        |                               |   | 1952.8                          |        |        |
| CCH  | 1845.8                        |                               |   |                                 |        |        |
| CCH <sup>+</sup>                                 | 1820.4                        |                               |   |                                 |        |        |
| Pd(C <sub>2</sub> H <sub>2</sub> )               | 1716.7                        |                               | 1716.7                                      | 1649.8                          |        |        |
| Pd(C <sub>2</sub> H <sub>2</sub> )               | 1709.8                        | 1583.1                        | 1651.8                                      | 1709.8                          | 1641.8 | 1583.1 |
| Pd(C <sub>2</sub> H <sub>2</sub> )               | 1707.4                        |                               |   | 1707.4                          | 1638.8 |        |
| Pd <sub>2</sub> (C <sub>2</sub> H <sub>2</sub> ) | 1572.7                        | 1506.4                        | 1572.7                                      | 1521.5                          |        |        |
| Pd <sub>2</sub> (C <sub>2</sub> H <sub>2</sub> ) | 1565.8                        |                               |   |                                 |        |        |
| Pd <sub>2</sub> (C <sub>2</sub> H <sub>2</sub> ) | 989.6                         |                               |   |                                 |        |        |
| Pd <sub>2</sub> (C <sub>2</sub> H <sub>2</sub> ) | 985.7                         |                               |   |                                 |        |        |
| Pd(HD)   |                               |                               |   | 804.1                           |        |        |
| C <sub>x</sub> H <sub>y</sub>                    | 926.5                         |                               | 916.8                                       |                                 |        |        |
| C <sub>x</sub> H <sub>y</sub>                    | 893.5                         |                               | 887.5                                       |                                 |        |        |
| C <sub>x</sub> H <sub>y</sub>                    | 855.5                         |                               | 847.9                                       |                                 |        |        |
| C <sub>x</sub> H <sub>y</sub>                    | 853.1                         |                               | 845.2                                       |                                 |        |        |
| Pd(C <sub>2</sub> H <sub>2</sub> )               | 765.8                         |                               |   |                                 |        |        |
| Pd(C <sub>2</sub> H <sub>2</sub> )               | 764.5                         |                               | 756.1                                       |                                 |        |        |
| Pd(C <sub>2</sub> H <sub>2</sub> )               | 675.4                         |                               | 672.3                                       |                                 |        |        |
| Pd(C <sub>2</sub> H <sub>2</sub> )               | 674.5                         |                               | 671.5                                       |                                 |        |        |

<sup>a</sup> Frequencies are all measured in cm<sup>-1</sup>. Assignments from previous work on reaction of Pd atoms with acetylene.<sup>18</sup>

**TABLE 5: Observed Frequencies for Reaction Products Other than the Insertion Complex of Pt and Ethylene<sup>a</sup>**

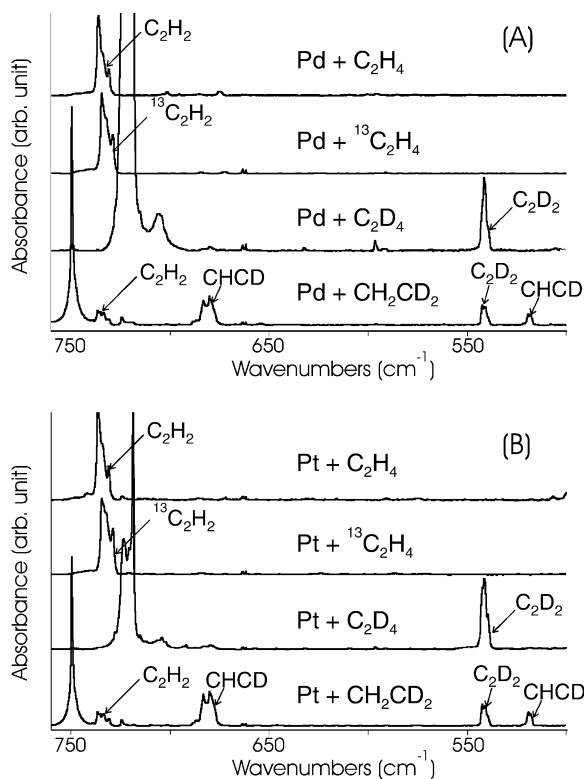
| species             | C <sub>2</sub> H <sub>4</sub> | C <sub>2</sub> D <sub>4</sub> | <sup>13</sup> C <sub>2</sub> H <sub>4</sub> | CH <sub>2</sub> CD <sub>2</sub> |        |
|---------------------|-------------------------------|-------------------------------|---|---------------------------------|--------|
| PtCCH               | 2016.2                        |                               |   | 2016.2                          |        |
| PtCCH <sup>-</sup>  | 1920.5                        |                               |   | 1920.5                          |        |
| CCH                 | 1845.8                        | 1746.5                        | 1785.5                                      | 1845.8                          | 1746.5 |
| CCH <sup>+</sup>    | 1724.4                        |                               | 1754.9                                      | 1724.4                          |        |
| Pt–CCH <sub>2</sub> | 1716.5                        | 1662.6                        |   | 1716.5                          |        |

<sup>a</sup> Frequencies are all in cm<sup>-1</sup>. Assignments are assisted by the results of previous work done on the reaction of Pt atoms with acetylene.<sup>19</sup>

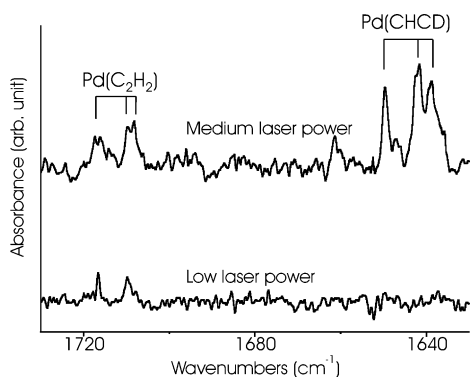
indicates that the Pt–acetylene  $\pi$  complexes are not formed as readily as the corresponding Pd–acetylene complexes, which is consistent with our previous results on the reactions of Pd and Pt atoms with acetylene.<sup>18,19</sup> We anticipate that some of the C<sub>2</sub>H<sub>2</sub> observed here, and its CCH photolysis product, are produced by VUV photodissociation of C<sub>2</sub>H<sub>4</sub> from the ablation plume; however, the large yield of C<sub>2</sub>H<sub>2</sub> invites the consideration of additional reaction mechanisms. Furthermore, our CH<sub>2</sub>CD<sub>2</sub> experiments give C<sub>2</sub>H<sub>2</sub> and C<sub>2</sub>D<sub>2</sub> in addition to the dominant CHCD product, although some product scrambling is observed in the VUV photochemistry of CH<sub>2</sub>CD<sub>2</sub>.<sup>31</sup> Acetylene produced in large quantity suggests that hydrogen is also eliminated from ethylene in the reaction of laser-ablated metal atoms and ethylene, a point advanced earlier for Zr + C<sub>2</sub>H<sub>4</sub> reactions.<sup>33</sup> Hydrogen elimination reactions of ethylene by transition-metal atoms have recently drawn broad attention, in particular, the activities of the early second-row transition-metal atoms have been the subject of intense studies.<sup>16,17,26,27,32,33</sup> However, such reactions by the late transition metals have not been closely examined to date.<sup>34</sup>

Figure 7 shows the Pd(C<sub>2</sub>H<sub>2</sub>) and Pd(CHCD) complexes formed in the reaction of Pd and CH<sub>2</sub>CD<sub>2</sub>: a weak Pd(C<sub>2</sub>D<sub>2</sub>) complex band was also observed at 1583.1 cm<sup>-1</sup>. The frequencies observed here are 0.2–0.3 cm<sup>-1</sup> higher than those found in the C<sub>2</sub>H<sub>2</sub> investigation,<sup>18</sup> which is close enough to confirm that the same complexes are formed.

We observe more Pd(C<sub>2</sub>H<sub>2</sub>) relative to Pd(CHCD) at medium laser power than the 1:5 distribution of C<sub>2</sub>H<sub>2</sub> and CHCD would give if these Pd complexes were formed only from the acetylene



**Figure 6.** IR spectra in the region of 500–800  $\text{m}^{-1}$  for laser-ablated Pd (A) and Pt (B) atoms codeposited with ethylene isotopomers diluted in argon at 7 K. The acetylene  $\pi_u$  absorptions for the isotopomers are indicated.



**Figure 7.** IR spectra in the 1630–1730  $\text{cm}^{-1}$  region for laser-ablated Pd codeposited at 7 K with  $\text{CH}_2\text{CD}_2$  in excess argon using low laser power and medium laser power.

isotopomers. At low laser power, we observe only  $\text{Pd}(\text{C}_2\text{H}_2)$ . How might we account for this in the reaction of  $\text{Pd}^*$  and  $\text{CH}_2\text{CD}_2$ ? This suggests an energized  $\text{Pd}(\text{CH}_2\text{CD}_2)^*$  intermediate, which eliminates the most stable isotopic dihydrogen: this is  $\text{D}_2$  (dissociation energy of  $\text{D}_2$  is 1.8 kcal/mol higher than that for  $\text{H}_2$ ).<sup>35</sup> In addition,  $\text{Pd}(\text{HD})$  is observed, which could come from reaction 3b.

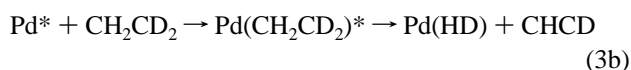


Figure 6 shows the strong  $\pi_u$  absorptions of free acetylene isotopomers, the final products of hydrogen elimination of ethylene isotopomers. It is notable that  $\text{C}_2\text{H}_2$  and  $\text{C}_2\text{D}_2$  as well as CHCD are generated as reaction products of hydrogen elimination of  $\text{CH}_2\text{CD}_2$ . The estimated molar ratio between

$\text{C}_2\text{H}_2$ , CHCD, and  $\text{C}_2\text{D}_2$  produced in the reaction, using the calculated absorption intensities of the  $\pi_u$  bands of the isotopomers, is about 1:5:2, essentially the same for both Pd and Pt. This result is consistent with our previous hydrogen elimination reaction of ethylene by zirconium, an early second-row transition metal.<sup>20</sup> The currently accepted reaction path for the hydrogen elimination reaction does not allow the formation of  $\text{C}_2\text{H}_2$  or  $\text{C}_2\text{D}_2$  from  $\text{CH}_2\text{CD}_2$  because one hydrogen atom is supposed to depart from each carbon atom.<sup>32</sup> This mechanism was proposed for the reaction between thermalized metal atoms and ethylene; our laser-vaporized metal atoms have much higher kinetic and possibly electronic energy. However, the current reaction mechanism has not been tested with  $\text{CH}_2\text{CD}_2$  in reaction dynamics. Obviously, further studies are needed to examine more closely the details of the hydrogen extraction reaction of ethylene by transition metals.

## Conclusions

Reactions of laser-ablated palladium and platinum atoms with ethylene isotopomers have been carried out in excess argon during condensation at 7 K. Evidence shows that the Pd atom forms a  $\pi$  complex with ethylene. The  $\text{C}=\text{C}$  stretching mode, which is originally IR inactive for ethylene, becomes active upon formation of the  $\pi$  complex, but the intensity is still very low. The Pt atom, however, forms an insertion product with ethylene, and the polarized  $\text{C}=\text{C}$  bond results in many strong IR absorptions, particularly the 1559.7  $\text{cm}^{-1}$  band, which is the strong  $\text{C}=\text{C}$  stretching mode of the complex as a result of the  $\text{C}-\text{H}$  insertion. This contrasting behavior for Pd and Pt with  $\text{C}_2\text{H}_4$  is analogous to their reactions with  $\text{H}_2$  to form the  $\text{Pd}(\text{H}_2)$  complex and  $\text{PtH}_2$  dihydride.<sup>29,30</sup>

Other reaction products are also generated, especially acetylene, which is the final product of the  $\text{H}_2$  elimination reaction of ethylene by metal atoms, and other weak absorptions arise from acetylene complexes. In this context, the  $\pi$  and insertion complexes are in fact reaction intermediates, and the presence of those complexes indicates where high-energy barriers lie in the  $\text{H}_2$  elimination reaction path. Finally,  $\text{C}_2\text{H}_2$  and  $\text{C}_2\text{D}_2$  are formed along with CHCD in the reactions of  $\text{CH}_2\text{CD}_2$  with Pd and Pt, which are not allowed in the currently accepted  $\text{H}_2$  elimination reaction path, suggesting that the reaction occurs in more than one step or follows a different route.

**Acknowledgment.** We gratefully acknowledge financial support for this work from NSF grant CHE 00-78836 and sabbatical leave support (H.-G.C.) from the Korea Research Foundation (KRF-2003-013-C00044).

## References and Notes

- (1) Mitchell, S. A.; Simard, B.; Rayner, D. M.; Hackett, P. A. *J. Phys. Chem.* **1988**, *92*, 1655.
- (2) Mochida, K.; Hirahue, K.; Suzuki, K. B. *Chem. Soc. Jpn.* **2003**, *76*, 1023 and references therein.
- (3) Cristian, A.-M. C.; Krylov, A. I. *J. Chem. Phys.* **2003**, *118*, 10912.
- (4) Manceron, L.; Hawkins, M.; Andrews, L. *J. Phys. Chem.* **1986**, *90*, 4987.
- (5) Merle-Mejean, T.; Cosse-Mertens, C.; Bouchareb, S.; Galan, F.; Mascetti, J.; Tranquille, M. *J. Phys. Chem.* **1992**, *96*, 9148.
- (6) Ozin, G. A.; Power, W. J. *Inorg. Chem.* **1977**, *16*, 212.
- (7) Huber, H.; Ozin, G. A.; Power, W. J. *Inorg. Chem.* **1977**, *16*, 979.
- (8) Lee, Y. K.; Hannachi, Y.; Xu, C.; Andrews, L.; Manceron, L. *J. Phys. Chem.* **1996**, *100*, 11228.
- (9) Manceron, L.; Andrews, L. *J. Phys. Chem.* **1989**, *93*, 2964.
- (10) Huber, H.; Ozin, G. A.; Power, W. J. *J. Am. Chem. Soc.* **1976**, *98*, 6508.
- (11) Ozin, G. A.; Power, W. J. *Inorg. Chem.* **1977**, *16*, 2864.
- (12) Lee, Y. K.; Manceron, L. *J. Mol. Struct.* **1997**, *415*, 197.

- (13) Paper presented at conference quoted in Rytter, E.; Gruen, D. M. *Spectrochim. Acta, Part A* **1979**, 35, 199.
- (14) Koszinowski, K.; Schöder, D.; Schwarz, H. *Organometallics* **2003**, 22, 3809.
- (15) Chantson, J.; Gorls, H.; Lotz, S. *J. Organomet. Chem.* **2003**, 687, 39.
- (16) Siegbahn, P. E. M.; Blomberg, M. R. A.; Svensson, M. *J. Am. Chem. Soc.* **1993**, 115, 1952.
- (17) Blomberg, M. R. A.; Siegbahn, P. E. M.; Svensson, M. *J. Phys. Chem.* **1992**, 96, 9794.
- (18) Andrews, L.; Wang, X. *J. Phys. Chem. A* **2003**, 107, 337 (Pd + C<sub>2</sub>H<sub>2</sub>).
- (19) Wang, X.; Andrews, L. *J. Phys. Chem. A* **2004**, 108, 4835. (Pt + C<sub>2</sub>H<sub>2</sub>).
- (20) Cho, H.-G.; Andrews, L. *J. Phys. Chem. A* **2004**, 108, 3965. (Zr + C<sub>2</sub>H<sub>4</sub>).
- (21) Zhou, M. F.; Andrews, L.; Bauschlicher, C. W., Jr. *Chem. Rev.* **2001**, 101, 1931.
- (22) Andrews, L.; Zhou, M.; Chertihin, G. V.; Bauschlicher, C. W., Jr. *J. Phys. Chem. A* **1999**, 103, 6525.
- (23) Burkholder, T. R.; Andrews, L. *J. Chem. Phys.* **1991**, 95, 8697.
- (24) Hassanzadeh, P.; Andrews, L. *J. Phys. Chem.* **1992**, 96, 9177.
- (25) Frisch, M. J.; Trucks, G. W.; Schlegel, H. B.; Scuseria, G. E.; Robb, M. A.; Cheeseman, J. R.; Zakrzewski, V. G.; Montgomery, J. A., Jr.; Stratmann, R. E.; Burant, J. C.; Dapprich, S.; Millam, J. M.; Daniels, A. D.; Kudin, K. N.; Strain, M. C.; Farkas, O.; Tomasi, J.; Barone, V.; Cossi, M.; Cammi, R.; Mennucci, B.; Pomelli, C.; Adamo, C.; Clifford, S.; Ochterski, J.; Petersson, G. A.; Ayala, P. Y.; Cui, Q.; Morokuma, K.; Malick, D. K.; Rabuck, A. D.; Raghavachari, K.; Foresman, J. B.; Cioslowski, J.; Ortiz, J. V.; Stefanov, B. B.; Liu, G.; Liashenko, A.; Piskorz, P.; Komaromi, I.; Gomperts, R.; Martin, R. L.; Fox, D. J.; Keith, T.; Al-Laham, M. A.; Peng, C. Y.; Nanayakkara, A.; Gonzalez, C.; Challacombe, M.; Gill, P. M. W.; Johnson, B. G.; Chen, W.; Wong, M. W.; Andres, J. L.; Head-Gordon, M.; Replogle, E. S.; Pople, J. A. *Gaussian 98*, revision A.11.4; Gaussian, Inc.: Pittsburgh, PA, 1998.
- (26) Willis, P. A.; Stauffer, H. U.; Hinrichs, R. Z.; Davis, H. F. *J. Phys. Chem. A* **1999**, 103, 3706.
- (27) Porembski, M.; Weisshaar, J. C. *J. Phys. Chem. A* **2001**, 105, 6655.
- (28) Lee, Y. K.; Manceron, L.; Papai, I. *J. Phys. Chem. A* **1997**, 101, 9650.
- (29) Andrews, L.; Wang, X.; Alikhani, M. E.; Manceron, L. *J. Phys. Chem. A* **2001**, 105, 3052.
- (30) Andrews, L.; Wang, X.; Manceron, L. *J. Chem. Phys.* **2001**, 114, 1559.
- (31) Chang, A. H. H.; Mebel, A. M.; Yang, X.-M.; Lin, S. H.; Lee, Y. T. *J. Chem. Phys.* **1998**, 109, 2748.
- (32) Porembski, M.; Weisshaar, J. C. *J. Phys. Chem. A* **2001**, 105, 4851.
- (33) (a) Wen, Y.; Porembski, M.; Ferrett, T. A.; Weisshaar, J. C. *J. Phys. Chem. A* **1998**, 102, 8362. (b) Porembski, M.; Weisshaar, J. C. *J. Phys. Chem. A* **2000**, 104, 1524.
- (34) Carroll, J. J.; Haug, K. L.; Weisshaar, J. C.; Blomberg, M. R. A.; Siegbahn, P. E. M.; Svensson, M. *J. Phys. Chem.* **1995**, 99, 13955.
- (35) Huber, K. P.; Herzberg, G. *Constants of Diatomic Molecules*; Van Nostrand: Princeton, NJ, 1979.